Journal of Radioanalytical and Nuclear Chemistry (2024) 333:495–518
https://doi.org/10.1007/s10967-023-09228-1

Geology of the Tamusu clay site for high level waste

Hongxia Gao[1] · Guangrong Li[1] · Xiaodong Liu[1] · Zheng Rao[1,2] · Pinghui Liu[1] · Honghui Li[3] · Shuai Liu[1] · Zhijun Gong[1] · Fengjuan Ni[1]

Received: 29 August 2023 / Accepted: 19 October 2023 / Published online: 4 November 2023

Abstract
Tamusu area in Inner Mongolia is a candidate site for the first clay rock repository in China. Comprehensive analyses conducted on stratigraphic characteristics, mineralogy, structural geology, and three-dimensional geological modeling in the Tamusu area showed that: the thickness of clay rock is more than 200 m with burial depth ranging from 200 to 800 m, which is mainly composed of zeolite, dolomite, and illite. Fractures are not well developed and the tectonic environment is stable. Additionally, the terrain and landform are relatively flat and desolate. These findings suggest that the Tamusu area presents favorable geological conditions for the construction and operation of a high-level radioactive waste repository.

Keywords Clay rock · Fault stability · High-level radioactive waste geological disposal · Tamusu

Introduction

When selecting a site for high-level radioactive waste disposal repository, the type of host rock is an essential factor to consider. Countries with nuclear power worldwide have studied various host rock types, including granite, mudstone (clay rock), and salt rock. There are currently several underground research laboratories worldwide that explore different types of host rocks for high-level radioactive waste disposal. Of these host rocks, granite and clay rock are widely studied as repositories [1, 2]. France, Belgium, Switzerland, Japan, Hungary, Spain, and other countries have explored potential sites for clay rock repositories. Among them, France, Switzerland, and Belgium have made significant progress in research and development related to clay rock repositories due to their advanced technical level. Some of the international underground laboratories for the geological disposal of high-level radioactive waste in claystone include the CenterMeuse/Haunt Marn and Tournemire underground laboratories in France, the Mont Terri underground laboratory in Switzerland, and the Mol underground laboratory in Belgium.

In China, clay rock has emerged as a potential candidate host rock for high-level radioactive waste geological repositories [2–7]. A preliminary study on the geological environment of thick-layered clay rocks in mainland China was conducted through geological survey and data collection (Fig. 1), which indicated that Gansu Longdong, the South Baxian area of Chaidamu Basin, and the Bayin Gobi Basin of Inner Mongolia represent key investigation areas for follow-up work. In 2014, a preliminary suitability evaluation was performed for key survey areas, including the Bayingobi, Tamusu, and Suhongtu regions, based on site selection criteria of clay rock, geological conditions, socio-economic factors, and drilling resources [8–10]). The drilling project of the China high-level radioactive waste clay rock geological repository project was launched in 2017, with the TZK-1 and TZK-2 drilling projects carried out in the Tamusu research area. In 2018, the clay rock section in the Tamusu region was screened and evaluated, leading to the identification of Tamusu as the preferred research area for the clay rock repository and the recommendation of two favorable sections.

✉ Guangrong Li
liguangrong0086@ecut.edu.cn

Hongxia Gao
hxgao@ecut.edu.cn

[1] State Key Laboratory of Nuclear Resources and Environment, East China University of Technology, Nanchang 330013, Jiangxi, China

[2] Jiangxi Provincial Institute of Nuclear Geology (Jiangxi Nuclear Geological Bureau 266th Brigade), Nanchang 330038, Jiangxi, China

[3] China Institute for Radiation Protection, Taiyuan 030006, Shanxi, China

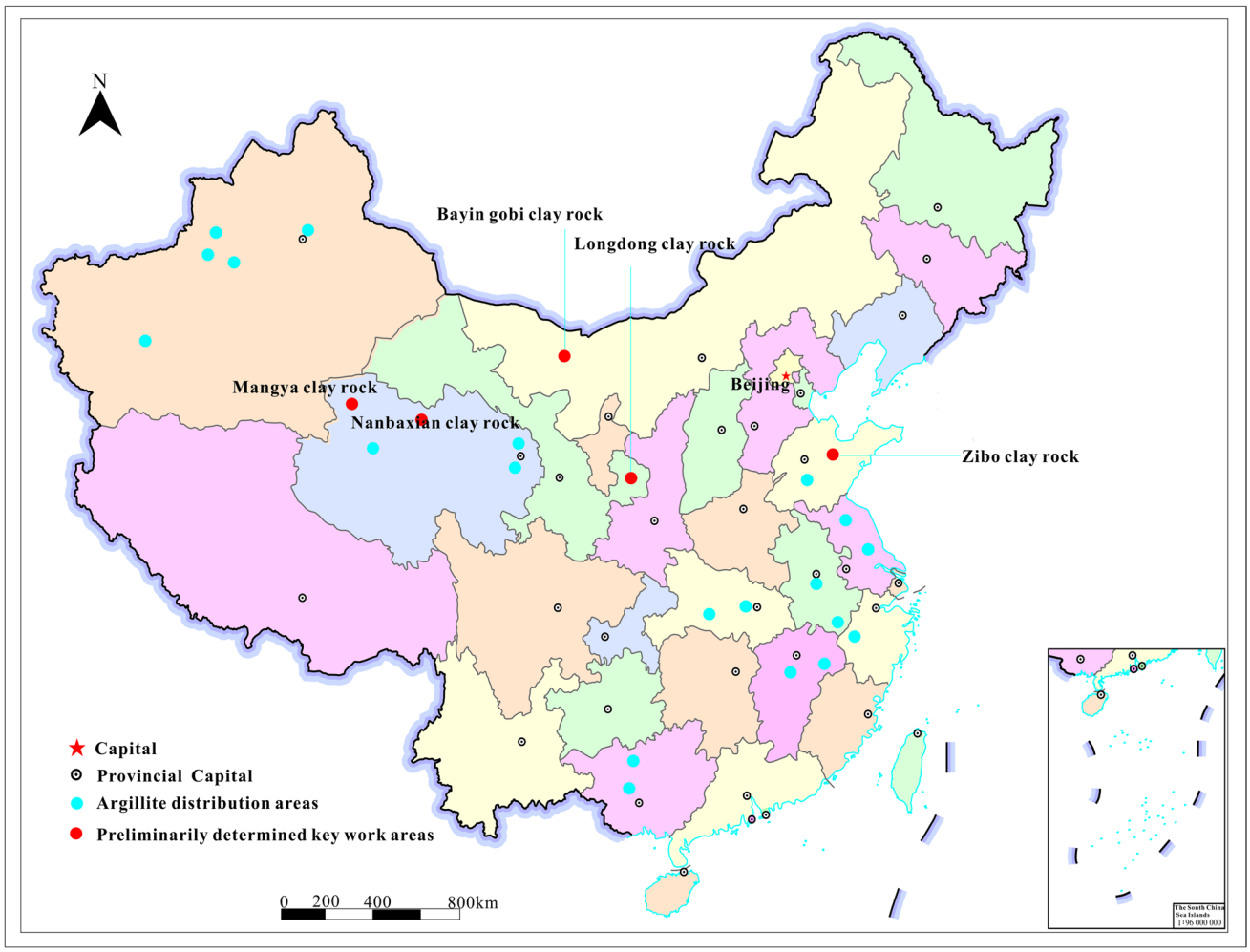

Fig. 1 Main clay rock candidates areas in China

When considering the long-term safety of radioactive waste disposal, clay rock is a potential host rock due to its low hydraulic conductivity, low solubility, strong adsorption to nuclides, and strong self-healing ability of plastic clay. The low hydraulic conductivity of clay rocks helps to delay the entry of radionuclides into the environment after the repository has been closed. In case of any radionuclide release from the repository, the strong adsorption of clay rock can keep most of the radionuclides within a certain range, thereby reducing the scope and degree of influence. Clay rock is typically a continuous porous medium, making it easier to carry out testing, evaluations, and predictions on groundwater flow and nuclide migration. This helps in reducing uncertainty in long-term safety forecasts.

Physiography and geomorphology

Physiography

The terrain of the Tamasu research area is generally high in the northwest and low in the southeast. Because it is located in the Hexi Corridor, the Beishan uplift zone, the Alxa Plateau, the Alxa trough anticline and the Bayanhaote trough anticline in the western section of the Inner Mongolia Plateau, it belongs to the temperate arid region of the Mongxin Plateau. There are many deserts, with middle and low mountains, alternating high plains, Gobi, hills and lake basins. The general elevation is 1270–1330 m,

and the relative elevation is about 60 m. Most of the surface is covered by Quaternary sand and dunes, with a relative height of 10–20 m. The topography and landforms in the study area are mainly Gobi, hills and deserts. There is basically no surface runoff in the study area, with sparse vegetation and fragile ecology. The landforms in the territory are divided into 6 types: stony soil mid-mountain landform, stony soil mid-low mountain landform, stony soil low mountain hilly denudation landform, sand dune landform, sandy soil hill lowland and stony, stony gravel Gobi. The altitude is 1000–3500 m.

Geomorphology

The Tamusu research area is located on the northwest side of the Inner Mongolia Plateau, on the eastern edge of the Badain Jaran Desert. The landform of the Badain Jaran Desert is gentle, mainly composed of denuded low mountain remnants and inter-mountain depressions. According to the field investigation and interpretation of aerial photographs and satellite images, the landscape form of the Badain Jaran Desert is mainly the terrain generated by the force of wind. Except for a small area of quasi-plain bedrock and residual hills at the edge, the vast area is covered by sand dunes (Fig. 2).

The topography of Alxa and its adjacent areas is characterized by a landscape of alternating basins and mountains: The Western Beishan area is alternately distributed between high (middle) mountains and small intermountain basins, and the altitude of the mountains is usually about 1700 m; The southern corridor area is also alternately distributed between high (middle) mountains and small intermountain basins; The interior is dominated by the Gobi Desert, of which the Badain Jaran Desert is one of the four largest deserts in the world; In the north, there are Hongguer Mountain and Menggen Ula Mountain. The east is crossed by Zongnai Mountain and Salazha Mountain, with an altitude of about 1200 m. There are also Huahai Basin, Chaoshui Basin, Yabulai Basin and Yingen-Ejinaqi Basin in the area.

Stratigraphy

The clay rock in the Tamusu research area is produced in the upper member of the Lower Cretaceous Bayinggobi Formation. Drilling revealed that the thickness of this layer is more than 200 m, the continuous thickness is more than 100 m, and the burial depth is more than 500 m. The categories include mudstone and shale, but the main types are gray and dark gray massive mudstone or mudstone with a small amount of silt. The rock has good homogeneity, high degree of consolidation, and hard and compact structure.

The caprock in the preselected section is a set of continental sedimentary strata formed in the Mesozoic and Cenozoic. The main caprocks are the Quaternary (Q) strata, the Bayingobi Formation (K_1b) and Wulansuhai Formation (K_2w) in the Cretaceous (K) strata, and the Jurassic (J) strata [11–15]. (Fig. 3). Among them, the stratum of the Bayingobi Formation (K_1b) is divided into two layers: the upper member (K_1b^2) and the lower member (K_1b^1). The study shows that the stratum of the upper member (K_1b^2) of the Lower Cretaceous Bayingobi Formation can be subdivided into three rock members, namely the first member. The rock section ($K_1b^{2\text{-}1}$), the second rock section ($K_1b^{2\text{-}2}$) and the third rock section ($K_1b^{2\text{-}3}$) [16, 17], the first rock section ($K_1b^{2\text{-}1}$) is Mudstone target horizons in the study area. For details, see Table 1and Fig. 3.

In order to systematically understand the difference in the relative content of minerals in the vertical direction of mudstone. Taking Well TZK-2 (well depth of 800.6 m) as an example, a semi-quantitative analysis of mudstone in the upper part of the Bayin Gobi was carried out combined

Fig. 2 Physiography and geomorphology of Tamusu area

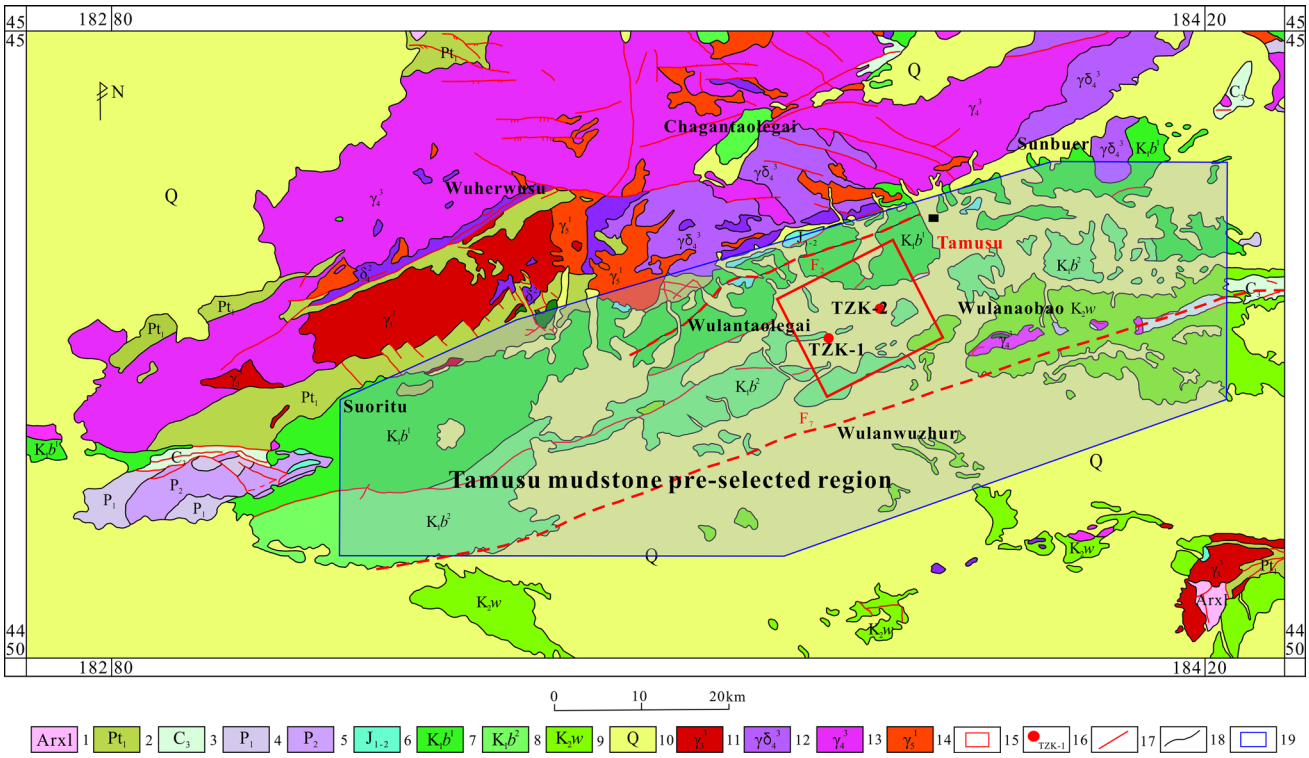

Fig. 3 Geological sketch of Tamusu mudstone preselected region. 1-Proterozoic Erathem; 2-Archean Erathem; 3-Carboniferous System; 4-Lower Permian; 5-Upper Permian; 6-Middle lower Jurassic; 7-Bayingobi formation Lower member of Lower Cretaceous; 8-Bayingobi formation Upper member of Lower Cretaceous; 9-Wulansuhai formation of Upper Cretaceous; 10-Quaternary; 11-Late Caledonian granite; 12-Middle Variscan gabbro; 13-Late Variscan granodiorite; 14-Late Variscan granite; 15-Indosinian granite; 16-faults; 17-Project borehole; 18-Borehole of nuclear industry 208; 19-Preselected region

with XRD diffraction technology (Fig. 4). It is found that the whole drilling mudstone is dominated by analcite, clay minerals (mainly illite) and carbonate minerals (mainly dolomite and ankerite). The upper mudstone (depth less than 528.77 m) is mainly zeolitic mudstone; the lower mudstone (depth greater than 550 m) is mainly dolomitic mudstone. Among them, the percentage of analite in the upper mudstone samples ranges from 20.1 to 61.5%, with the highest percentage between 550 and 600 m. The percentage of clay minerals ranges from 12.8 to 42.3%, mainly illite, with a small amount of montmorillonite and chlorite. The percentage of carbonate minerals (mainly dolomite and ankerite) ranges from 4.5 to 40.6%, with the highest percentage between 700 and 750 m with depth. The percentage of analite in the lower mudstone samples ranges from 2.7 to 40%, with the highest percentage between 550 and 600 m. The percentage of clay minerals ranges from 9.7 to 23.9%, and the percentage fluctuations are small, mainly illite, with a small amount of kaolinite and chlorite; The percentage of carbonate minerals (mainly dolomite and ankerite) ranges from 26.1 to 62.1%, with the highest percentage between 700 and 750 m with depth.

The comparison of the characteristic ratios of main oxides and rare earth elements in the study area can be found (Table 2). The main oxides of the upper and lower mudstones are SiO_2, CaO and Al_2O_3, and the three main oxides of the upper mudstone are slightly higher than those of the lower mudstone. The loss on ignition of major elements in the upper and lower mudstones is higher. It is speculated that it may be caused by the loss of structural water in carbonate or organic matter and clay minerals in the samples. It is speculated that the relatively high depletion of SiO_2 may be due to the fact that the SiO_2 in the upper mudstone samples of the upper Tamusu Bayingobi Formation mainly comes from silicate minerals. The enrichment of CaO in the samples indicates that the content of carbonate minerals in the minerals of the mudstone samples is relatively high. The weight of rare earth elements also varies greatly, but the average values are relatively close, and δEu and δCe show the same anomaly characteristics, that is, δEu is a moderately strong negative anomaly, while δCe is basically normal. In terms of trace elements, the upper and lower mudstones are obviously enriched in U and Sr, while Th, Co, Sc, Rb, Zr and Ba are depleted.

Table 1 Lithological characteristics table in Tamusu mudstone candidate sector

Strata						Depth (m)	Lithological features	Remarks
Erathem	Systerm	Series	Formation	Member	Units			
Cenozoic	Quaternary				Q	10	Widely distributed in the basin, the thickness is thin. Mainly gravel, aeolian sand, clay deposited in swamps or lakes deposited by rivers or alluvial fans, etc	
Mesozoic	Cretaceous	Upper	Wulansuhai formation		K_2w	> 200	It is widely distributed in the study area, and the contact mode with the underlying strata is angular unconformity. The upper part is mainly mudstone, brick red argillaceous siltstone and pebbly sandstone, with gypsum layer visible; The lower part is mainly brick red sandy conglomerate and conglomerate, with high argillaceous components	
		Lower	Bayin Gobi formation	Upper	K_1b^2	> 911	Part of the surface is exposed. The middle and lower parts of this layer develop brick red glutenite and khaki sandstone. Horizontal bedding is developed in the mudstone layer. Paging constructs appear locally. Mudstone and siltstone interbedded phenomenon can be seen	Target strata
				Lower	K_1b^1	1418	Exposed on the edge of the basin, the lithology is mainly thick gray-white conglomerate, dark gray glutenite sandwiched with thin mudstone and siltstone. A positive-grained structure can be seen on the sequence. The particle size is from fine to coarse. The lithology changes from sandstone to conglomerate	
	Jurassic	Lower snd Middle			J_{1-2}	4000	A small amount is distributed in the southwest and northeast of the Tamusu. The lithology is variegated glutenite with a small amount of limestone interlayers. The upper part is mainly gray-white and gray-black tuff. The lower part is mainly fine sandstone. Coal lines and shale interlayers can be seen. The contact relationship with the overlying and underlying strata is angular unconformity	

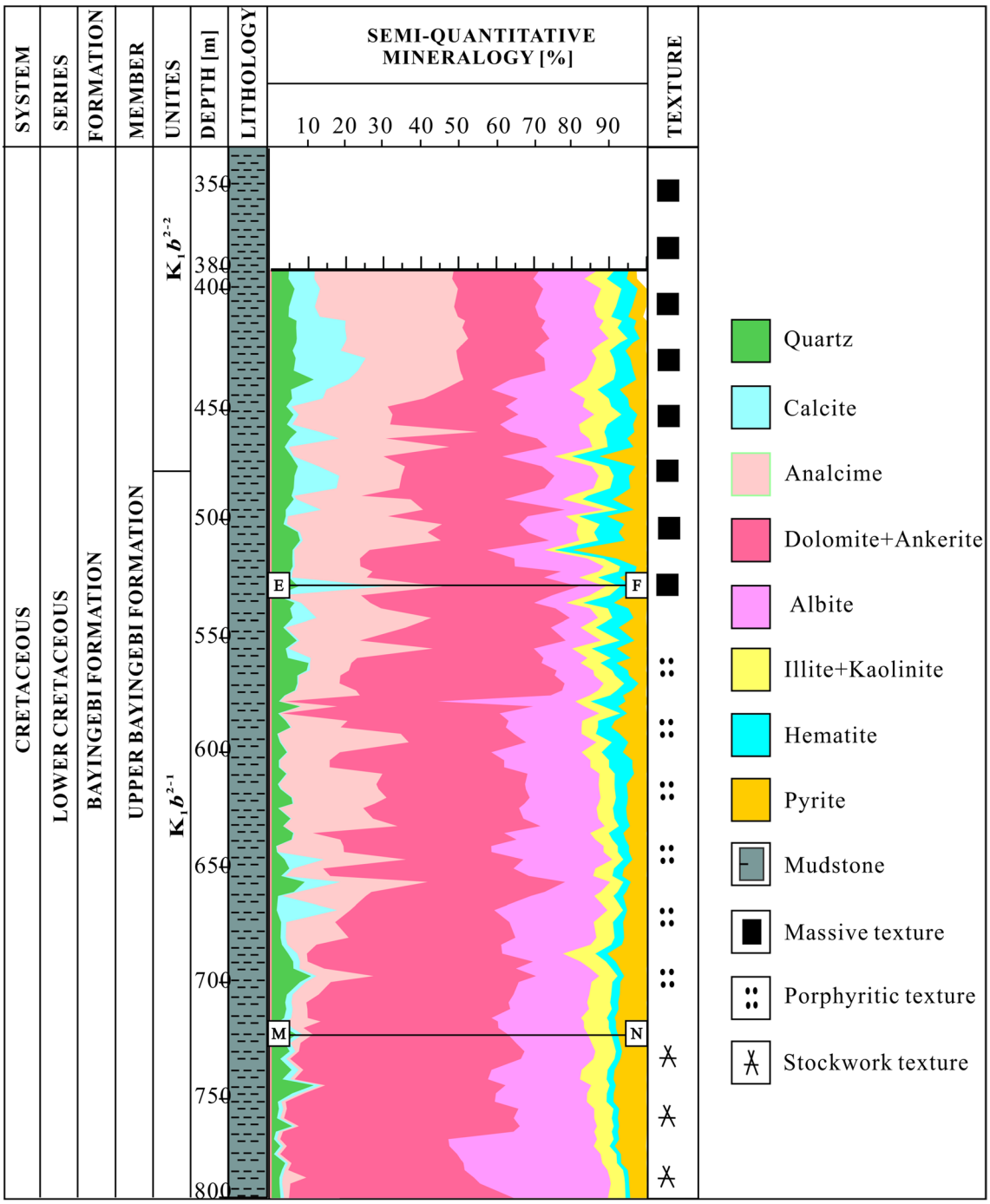

Fig. 4 Relationship between main constituent minerals of mudstone and sampling depth

The paleo-sedimentary environments of the upper and lower mudstone geochemical elements all indicate that the tectonic environments of the mudstone source areas are mainly continental island arcs and active continental margins. The crust above the parent rock is dominated by felsic rocks, mixed with medium-acid volcanic rocks. The Wenduer Maodao granodiorite and Tamusin diorite in the Zongnai Mountain-Shalazha Mountain area in the northern margin of the depression may be its main provenance. Vertically, the lower layer of the upper part of the Bayingobi Formation is arid, anaerobic, and strongly reducing salt lake environment. A distinct relatively wet and cold deposition process occurred in a hot and dry environment. Paleosalinity and redox environment are also coupled with dry–hot–cold–wet evolution. That is, there is a short-lived

Table 2 Comparison of geochemical characteristic elements

	Upper mudstone Range/average	Lower mudstone Range/average
SiO_2	19.58–53.6%/35.85%	18.80–45.05%/30.24%
CaO	2.37–28.5%/11.73%	5.33–19.55%/13.48%
Al_2O_3	4.65–17.74%/11.65%	11.26–16.42%/9.74%
Loss on ignition	5.77%–35.30%/19.30%	12.65%–32.13%/22.75%
∑REE	100.21–186.00 μg/g/130.60 μg/g	59.29–283.80 μg/g/129.49 μg/g
δEu	0.52–0.73/0.63	0.55–0.70/0.61
δCe	0.90–0.96/0.93	0.91–1.06/1

paleo-oxidative environment in the anaerobic, strongly reducing salt lake sedimentary environment.

Quaternary geology

Quaternary deposits are widely distributed in various depressions in the Bayin Gobi Basin, which are aeolian sand, alluvial, and alluvial sand-gravel layers. Drilling in the northern basin reveals that the thicknesses of the Tertiary and Quaternary are quite different; The Yabulai Mountains and the Harau Mountains in the southern basin are weakly thrust toward the basin due to the northward extrusion of the Indian plate.

General distribution and characteristics of surficial deposits

The Bayingobi Formation is widely distributed in the Tamusu area, and its distribution direction is NE. The sedimentary system is mainly composed of fan delta, braided delta and lacustrine sediments. Among them, the lacustrine sediments have a large area and are mainly distributed in the sedimentary centers of the secondary depressions. The lithology is dominated by gray, dark gray silty mudstone, mudstone intercalated with fine sandstone and siltstone. At the same time, lacustrine deposition is also an important condition for the formation of clay rocks in this area.

According to the field investigation and drilling data, the clay rock in the upper part of the Bayinggobi Formation in this area is produced in three layers, the upper, middle and lower layers (Fig. 5). The upper clay rock is mainly a set of lacustrine deposits (K_1b^{2-3}) with good continuity, with a thickness of 100–300 m, but the burial depth is shallow, generally ranging from several meters to tens of meters from the surface; The thickness of the middle clay rock layer is about tens of meters (K_1b^{2-2}), which is a set of fan-delta facies deposition, but its continuity is poor, often interbed with sandstone, and the thickness is relatively thin; The lower clay rock is a set of lacustrine thick clay rock layers (K_1b^{2-1}) with stable horizons and good continuity, mainly produced in the southwest of Tolgoi, Tamusu, and buried relatively deep. Existing boreholes reveal that this layer of clay rock has a buried depth more than 500 m and a continuous thickness more than 100 m, but all the current boreholes have not exposed the clay rock layer.

Erosion, deposition, and flooding

The research on the vertical dislocation and horizontal movement rate since the late Quaternary through the faults distributed in the Tamosin section shows that: The Sunbull fault (F_1 fault) was not very active in the late Quaternary. At the southern margin of Zongnai Mountain and Sharazha Mountain, about 3 km northeast of Tamusu, there are two river gullies across the Sunbuer fault, and late Quaternary river terraces developed on both sides of the gullies (Fig. 6a). There are several late Quaternary river terraces found in the Tamusin fault (F_2 fault), and these river terraces traverse the Tamusin fault. Using differential GPS to measure the river terrace platform, the results show (Fig. 6b) that the river terrace platform of the vertical F_2 fault is not continuous, and the natural erosion process caused the originally continuous river terrace to become discontinuous. The Ulantiebuke fault (F_4 fault) is clearly reflected in the aerial photographs, and the measurement results show that except for the local discontinuity of the alluvial fan caused by the erosion process (Fig. 6c). The Narenhara fault (F_7 fault) has no obvious vertical dislocation displacement in the vertical direction. Elevation measurements show that the overall plane is on a smooth surface, except for local discontinuities of the alluvial fan due to erosion processes (Fig. 6d).

Through analysis, it is identified that the depositional environment and depositional system of the upper and lower member of the Bayingobi Formation are quite different. During the deposition of the lower part of the Bayingobi Formation, the climate was arid and hot, and the sedimentary debris was generally red. Due to the influence of the strong activity of the basin margin faults, alluvial fan deposition is the main feature, and fan delta deposition appears in some sections. During the deposition of the upper member of the Bayingobi Formation, the climate changed fundamentally.

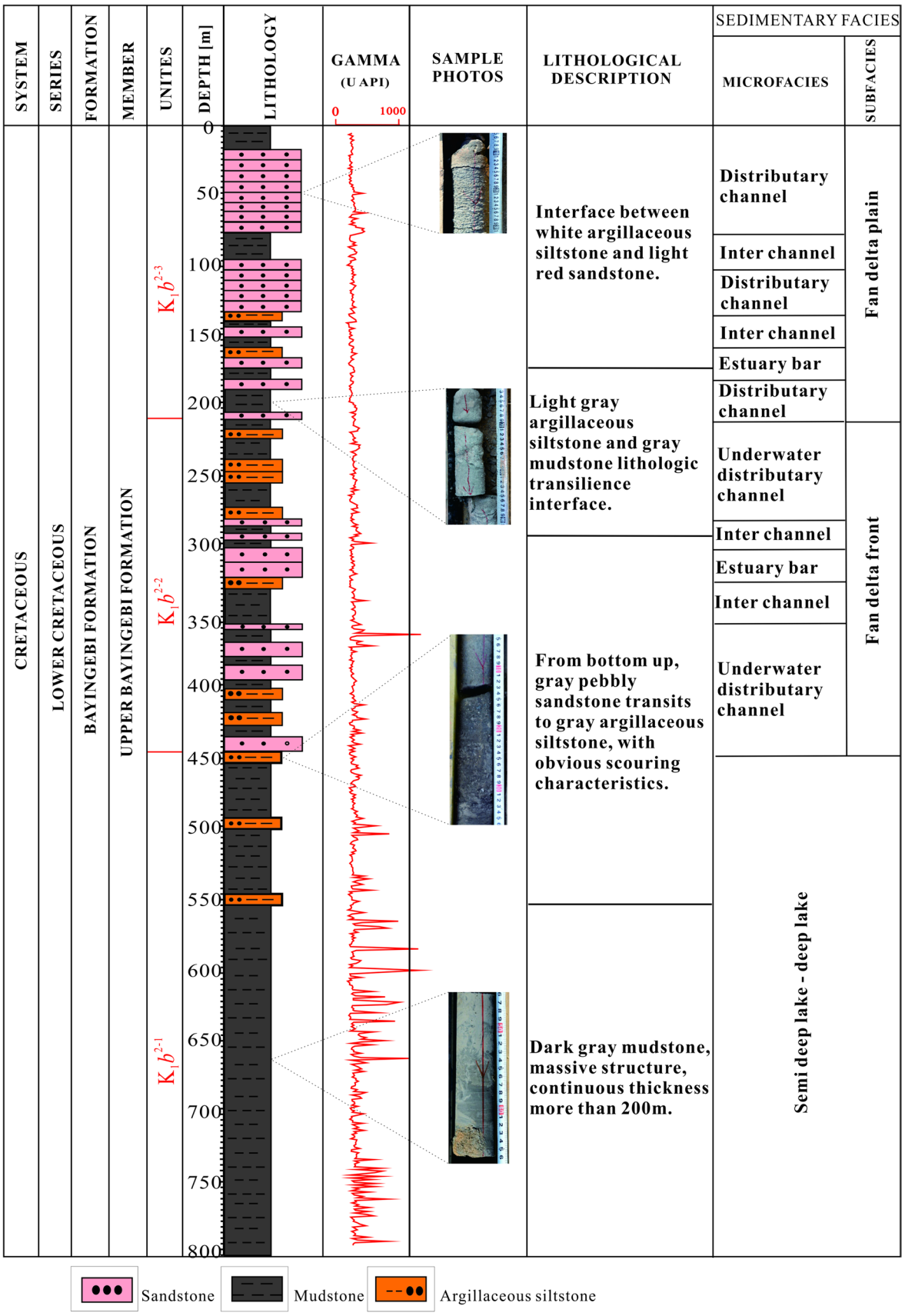

Fig. 5 Comprehensive histogram of sedimentary microfacies in borehole TZK-1

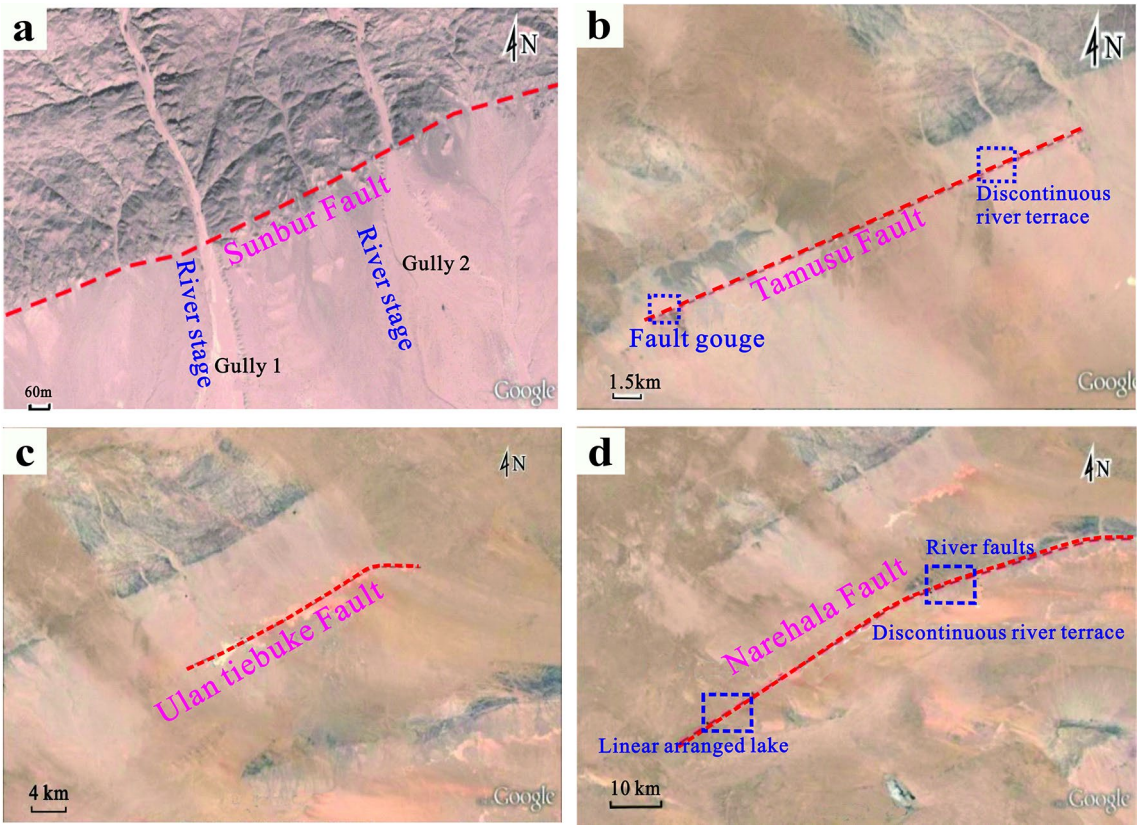

Fig. 6 Google Earth satellite image distribution map of the typical faults. **a** Sunbuer fault; **b** Discontinuous river terrace near Tamusin fault; **c** Dry lake along Ulan Tiebuke fault; **d** Narenhala compressive torsional fault

Fig. 7 Thick mudstone of shallow lacustrine sediments in the upper member of Bayingobi formation

From dry to wet, sedimentary debris is generally grey (Fig. 7). The lake basin experienced a rapid expansion, and the transporting action of flowing water was significantly enhanced. In addition to the original alluvial fan deposits and braided river delta deposits (Fig. 8), large-scale lacustrine deposits appeared.

Within the research scope of Tamusu, there has not been a large-scale flood disaster in the past 40 years. Even if it occurs occasionally, it is localized, indicating that the precipitation in the area will not cause disasters. At the same time, this area is located in the hinterland of the Asian continent, far away from the ocean, and is affected by the Mengxin high pressure and belongs to the desert and arid area. The water system and vegetation in the area are not developed. The water system is mostly seasonal currents and dry riverbeds.

Structural geology

The Tamusu study area is located in the Bayin Gobi Basin. The geological structure of the Bayin Gobi Basin is located at the transition between the Tianshan trough fold system and the North China platform. The southern part is the Langshan-Bayan Obo platform margin depression belt and the North China platform Alashan platform uplift. The northern part is the Tianshan trough fold system in the late Middle Beishan varix fold belt (Fig. 9).

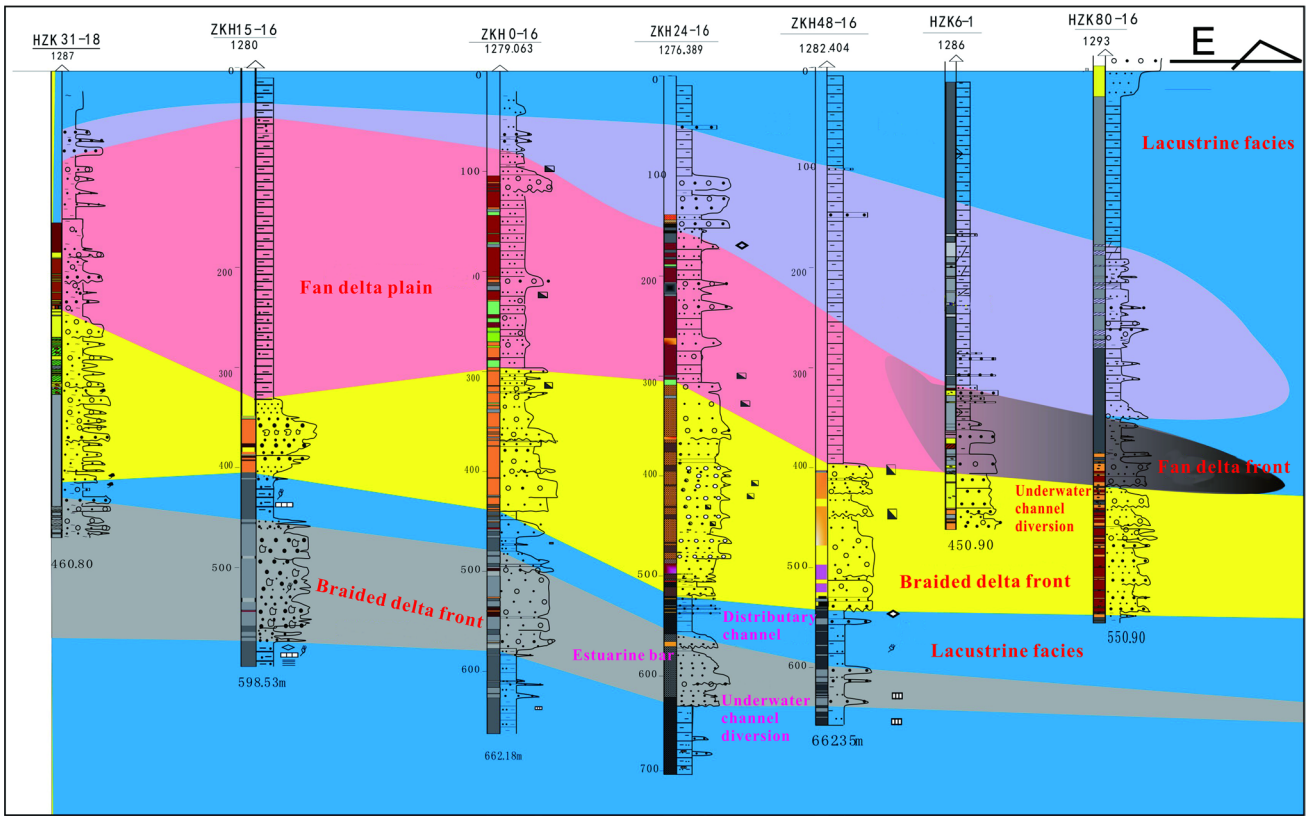

Fig. 8 Near east–west longitudinal section of the upper Bayingobi formation in tamusu section

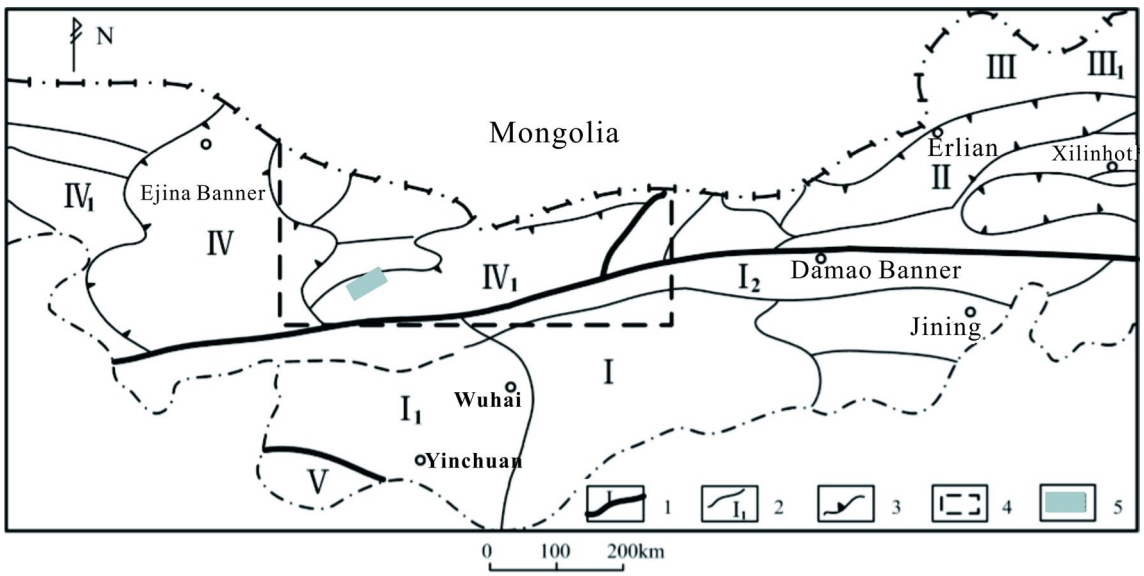

Fig. 9 Schematic diagram of tectonic unit division in central and Western Inner Mongolia. 1-Boundary and number of primary tectonic unit; 2-Boundary and number of secondary tectonic unit; 3-Meso Cenozoic continental basin; 4-Bayin Gobi Basin; 5-Work area; I-North China Platform; I_1-Alashan uplift; I_2-Langshan-Baiyunebo platform margin depression; II-Geosynclinal fold system of Middle Inner Mongolia; III-Xingmeng geosyncline fold system; III_1-East wuzhu early Variscan fold belt; IV-Tianshan geosyncline fold system; IV_1-Beishan late Variscan fold belt; V-Qilian Caledonian geosyncline fold system

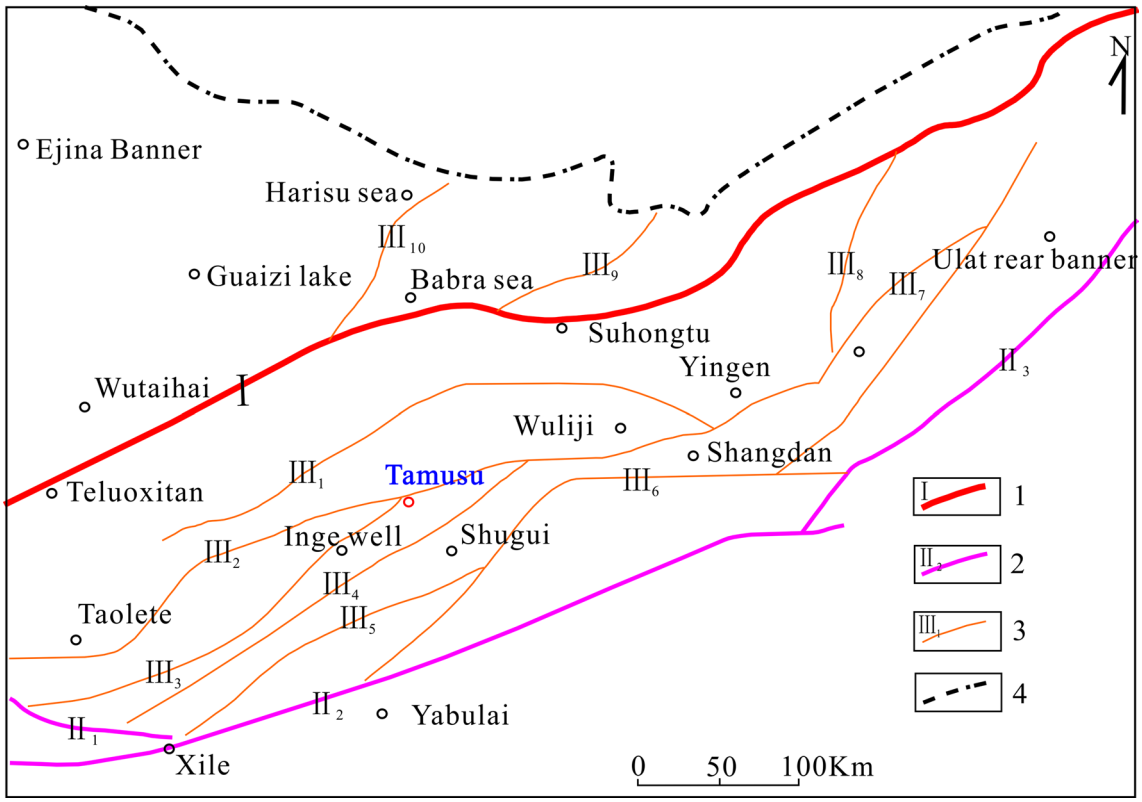

Fig. 10 Tectonic system map of the Bayingebi basin and its vicinities. 1-Regional major fault 2-Basin controlling fault 3-Intra Basin fault 4-Border

Faults

The research area of tamoxicin is at the junction between plates. From the perspective of regional geological evolution history, it has experienced complex and long-term tectonic movements, forming a series of complex fault tectonic systems. Based on the geological data, geophysical and satellite remote sensing data of the study area, and combined with previous research results [18–22], the study area A NEE-trending and NE-trending fault system is formed, and its main faults and secondary faults are intertwined with obvious characteristics (Fig. 10). According to the development characteristics and scale of faults in Tamunin and adjacent areas, the fault structures in the research area are mainly divided into three grades, namely: regional large faults (I), basin-controlling faults (II) and intra-basin faults (III).

Block-bounding faults

The Tamusu area is located in the Ingejing Depression of the Bayin Gobi Basin. There are relatively developed fault structures in the area, with concealed faults accounting for more than 80%. The fault activity period is mainly the Varixi period, followed by the Yanshan period and the Caledonian period. The Mesozoic and Cenozoic are mainly Yanshan faults, less Himalayan and Indosinian faults. According to its trend, it can be divided into three main fault systems. The most developed is the north-east-east direction, which often has the characteristics of long activity time, long extension, and large fault distance. It controls the tectonic and sedimentary development of the depression. Followed by north-west and east-west direction, very few are north-south direction, and the scale is small. The main basin-controlling faults include the northern Baoyintu fault, the Langshan fault, the Badainjilin fault, and the Zongnaishan-southern Shalazashan fault [23]. The main faults in the preselected section and all nearby areas are the Sunbuer fault (F_1 fault), the Tamusin fault (F_2 fault), the Wulan Taolgei fault (F_3 fault), the Ulan Tiebuke fault (F_4 fault), the Chaku fault Ertu fault (F_5 fault), Zhaganhaolai compressive torsional fault (F_6 fault), Narenhala compressive torsional fault (F_7 fault) and Badanjilin fault (F_8 fault). The fault structure is one of the important forms of tectonic activity in the area. The overall strike of its structural lines has two groups: NE-trending and near-EW-trending, near-EW-trending early and NE-trending late (Fig. 11) [14].

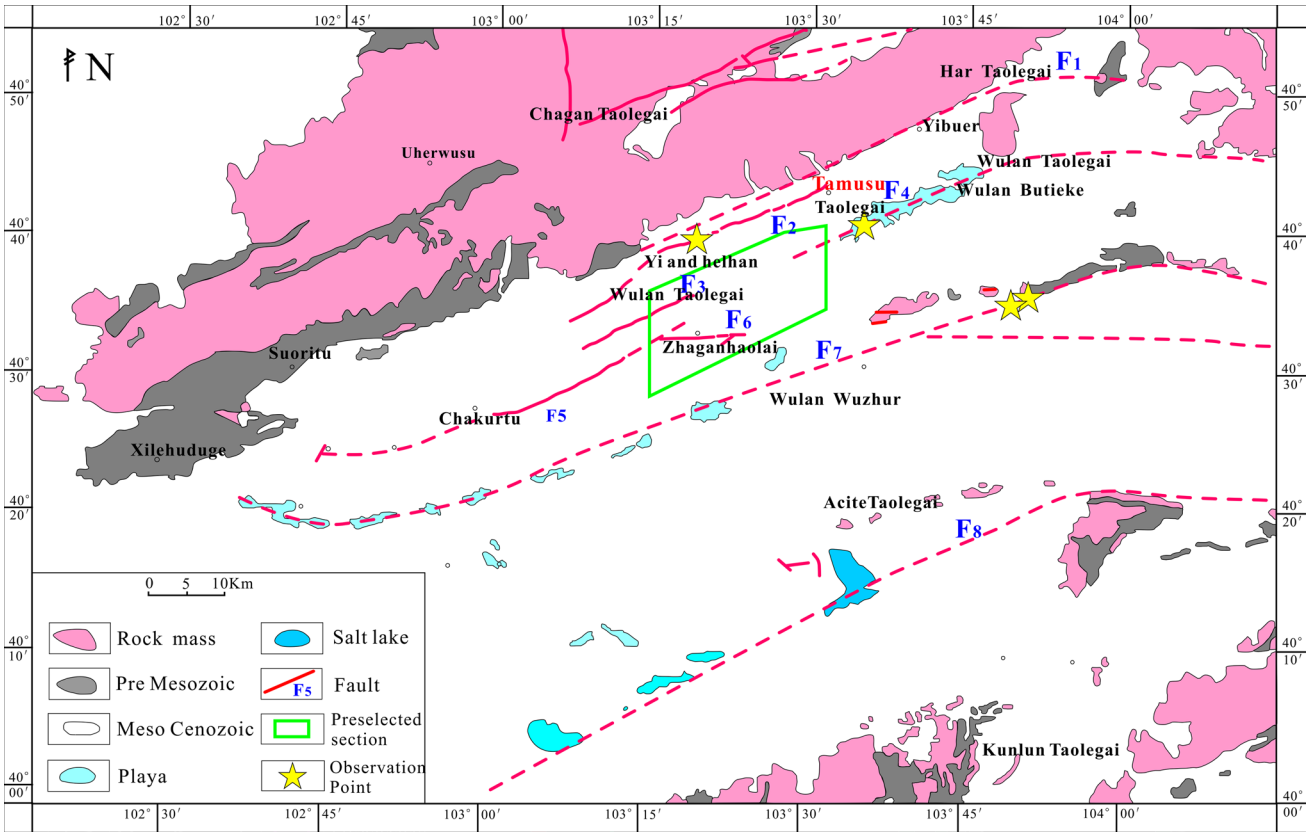

Fig. 11 Tectonic system map of Tamusu area

Structural blocks and intrablock faults

The first-level fault structure in the basin makes the basin form a structural pattern of uplift and depression, which controls the distribution of sedimentary facies and the composition of sedimentary systems. Secondary faults control the formation and distribution of depressions and elevations, and determine the local microscopic morphology of the spatial distribution of sedimentary facies. From the separation of plates in the Early Paleozoic to the collision of plates in the Late Ordovician, the plates were completely assembled at the end of the Late Paleozoic, and the dual basement of the folded basement and the Precambrian crystalline continental block was formed. The study area has always been on the passive continental margin and suture zone [24]. Starting from the Triassic, the basin entered the stage of intraplate structural deformation. The Early and Middle Triassic basins were in an orogenic uplift environment, and the Late Triassic study area entered a stage of crustal stretching and relaxation after the orogenic period, forming a set of NE-trending extensional fault systems [25, 26]. From the early Jurassic, under the influence of the Yanshan movement, the Tarim plate moved eastward relative to the Siberian plate, and under the influence of the left-lateral movement of the near-EW-trending strike-slip faults, a series of basin groups with obvious NE and NEE-trending pull points were formed [27]. Since the Early Cretaceous, the basin continued to be in an extensional tectonic environment, and a large number of normal faults developed on the basin margin. The study area has entered the full-scale development period of the pull-apart basin. Under the background of extension, the basin is expanded and connected into pieces, and the Early Cretaceous sediments are widely accepted. At the end of the Early Cretaceous, with the massive eruption of magma and the release of underground heat energy, the rifting and extension in the area was terminated, and the subsidence stage of the Yinzhang depression was entered. Since the Tertiary, the tectonic stress field of the basin in the study area has changed significantly due to the collision between the Indian plate and the Eurasian plate. From the early extension to the compression state, the basin is in the tectonic background of compression and uplift [28].

Table 3 Table of fracture elements in the Bayinggebi basin [8]

Fault number	Name	Property	Toward	Dip	Length (km)	Separation (km)
III1	Zongnai-salazha Mountain Fault	Reverse	EW	N	320	> 1500
III2	Zongnan fault	Normal	NE-EW	NW-N	> 500	
III3	Inge well fault	Normal	NE	SE	210	
III4	Shuhuaitou fault	Normal	NE		240	
III5	Yabulai Mountain ximi fault	Reverse	NE	SE	230	
III6	Narenhala fault	Reverse	NEE-EW	S-SSE	160	
III7	Desteura fault	Reverse	NEE	SSE	150	
III8	Amuwusu fault	Reverse	NE	SE	100	
III9	Daguxi fault	Normal	NNE	SSE	320	3600
III10	Dagudong fault	Normal	NNE	NWW	240	

There are 10 major faults in the basin. Its development characteristics and scales are different, and it is mainly distributed in the southern margin of the basin. These faults control the formation and distribution of depressions and uplifts in the basin, as well as the sedimentary characteristics, tectonic evolution and mineral accumulation of the basin. The fault location and structural elements are mainly shown in Table 3.

Fault activities

There are many active faults around Alxa, which have obvious features in tectonic landform, fault activity, crustal deformation, tectonic stress field, crustal structure, deep geophysical field, seismicity and so on. The main active faults around and inside Alxa include the Altyn active fault zone, the Langshan-Bayanwula active fault zone, the Helishan-Longshoushan Chagu active fault zone, the active fault zone on the northern margin of the Qilian Mountains, and the Yabulai Mountains active fault zone, active fault zone at the eastern foot of Helan Mountain, active fault zone at the western foot of Helan Mountain, Zhengyiguan active fault zone, Zhongwei active fault zone and Yingen active fault zone, etc.

Fault dislocation

The fault structures in the study area have obvious periods of movement, and the structural framework is strictly laid out. The F_1 and F_8 faults developed in the Late Jurassic, and they are the basin-controlling faults on the southern and northern margins of the basin in the working area. The F_2 and F_5 faults are a group of reverse thrust faults formed under the influence of the tectonic movement of the fifth episode of Yanshan at the end of the Late Cretaceous and under the action of compressive stress.

There are small folds in the west wall of the F_3 fault, which are two small anticlines with a strike of 70°–80°, and dip to the southwest. This fracture is an anti-torsional compressive torsional fault. The F_4 fault has a length of 65 km in the area. Most of the area is covered by the Quaternary, and only partially exposed in the Lower Cretaceous. The macroscopic distribution and geomorphological characteristics of the fault are clearly reflected in the aerial photos, and it is a compressive fault. The F_6 fault generally runs east–west, and the section dips steeply. The western section dips northward and the eastern section dips southward, and the fault develops in the Lower Cretaceous red bed. The fault cliff is developed, and the fault zone is generally in the shape of a gentle wave. There is a NE-trending compressive fault in the eastern segment of its southern pan, which may form a zigzag type with it, and the fault has a twisting property. The F_7 fault is an arc-shaped concealed fault that protrudes southward. Only in the late Carboniferous strata of Narenhala can clear structural traces be seen, resulting in straight and steep ridges in front of mountains or strip depressions in mountains. The fault bisected the Inge well depression (Fig. 12).

Earthquake

The Tamusu area belongs to the Alxa block, which is a rigid block. Since the Cenozoic, affected by the activity in the northern Qinghai-Tibet Plateau and the north-eastward activity of the Qilian Mountain orogenic belt in the southwest, the stronger seismic activity in this area is mainly distributed in the tectonic belt of the block boundary. The seismic activity inside the block is weak. According to the geological data of the study area, most of the faults in the area are covered by the overlying strata, and the surface exposure is not obvious, which brings great difficulties to

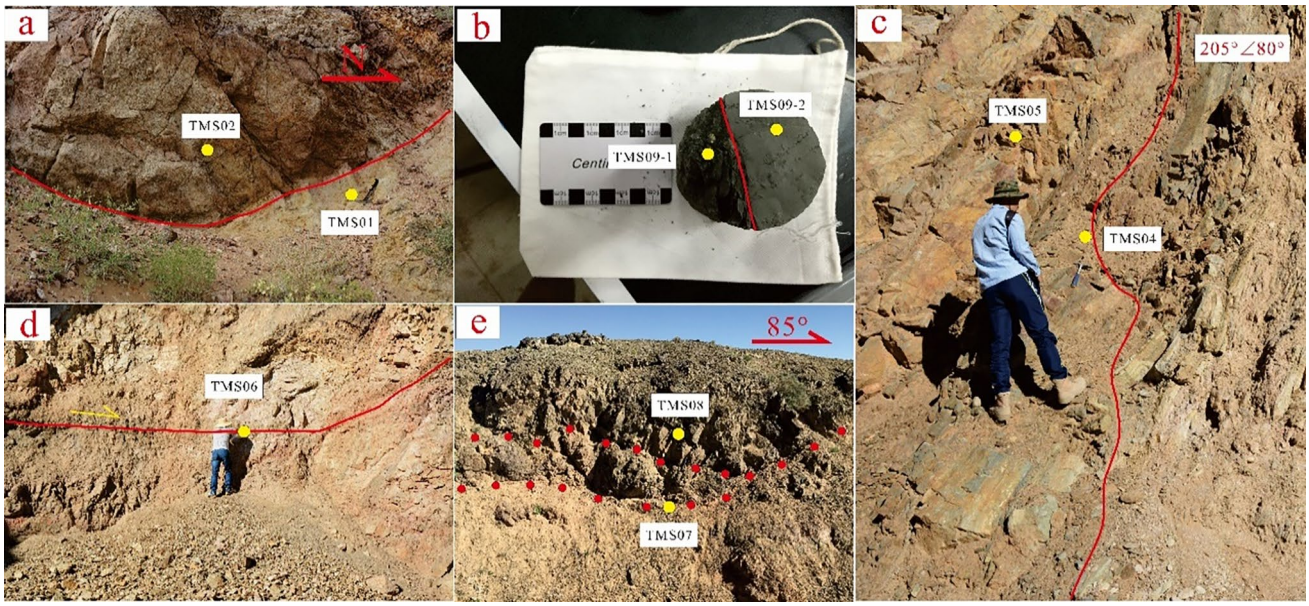

Fig. 12 Field outcrop of faults in Tamusu area. **a** F_2 fault; **b** F_4 fault; **c**–**e** F_7 fault

the evaluation of fault activity in the area. The most effective methods for the detection of hidden faults mainly include shallow seismic exploration, drilling and other methods, which can achieve the purpose of accurately locating active faults. This includes finding out important information such as the occurrence, distribution, and burial depth of hidden faults, which have been widely used in the detection of active faults in large cities [29, 30].

Combined with the previous work in this area (Fig. 13), the seismic time stacking profile and migration stacking time profile of each survey line in this region have a large number of reflected wave events. It has the characteristics of medium and weak amplitude, high frequency, strong phase, and good continuity [31], and meets the determination criteria for establishing a standard reflection layer. Combined with the geological data and borehole data in the Tamusu area, the super-sequence interface was determined by comparing, tracking and analyzing the seismic reflection data in the work area [32, 33], namely two standard reflection layers (T_3 and Tg), and 4 sequence interfaces (T_4, T_5, T_6 and T_7).

The corresponding relationship between each sequence interface and strata is shown in Table 4.

Generally speaking, the fault structures often lead to changes in the continuity of the rock or the original state of the formation. When a seismic wave passes through a fault, the propagation mode of the seismic wave at the fault will change due to the change of the propagation medium, such as diffraction. These faults often show dislocation or twisting of continuous seismic reflections on the seismic section, the similarity of their waveforms changes, and the continuity deteriorates [27]. Therefore, faults can be identified by using the variation characteristics of parameters such as the amplitude and phase of the emitted waves on the seismic emission profile [34]. According to the abnormal wave characteristics on the seismic reflection profile, it is inferred that there are 9 main structural faults in the working area, and their distribution is shown in Fig. 13.

The development characteristics of each fault can be judged according to the characteristics of the emission wave group on each seismic profile and the determined standard emission horizon (Fig. 14). The features of fault structures revealed by the L04 and L06 line sections of shallow seismic exploration are very clear. From the fault interpretation results of this shallow seismic section, it can be seen that the occurrence of stratigraphic interfaces has changed significantly near the fault. Combined with the geological structure characteristics of this area, 4 faults F_1, F_3, F_4, and F_7 with obvious characteristics are explained on the L04 seismic section, and 3 faults F_5, F_8 and F_9 with obvious characteristics are explained on the L06 seismic section. Combined with the other 9 seismic sections and geological interpretation sections, we can infer the development characteristics of fault structures in the working area (Table 5).

On the whole, the fault tectonic movement stages in the working area are obvious, and the structural framework layout is strict. The strike of most of the fault structures

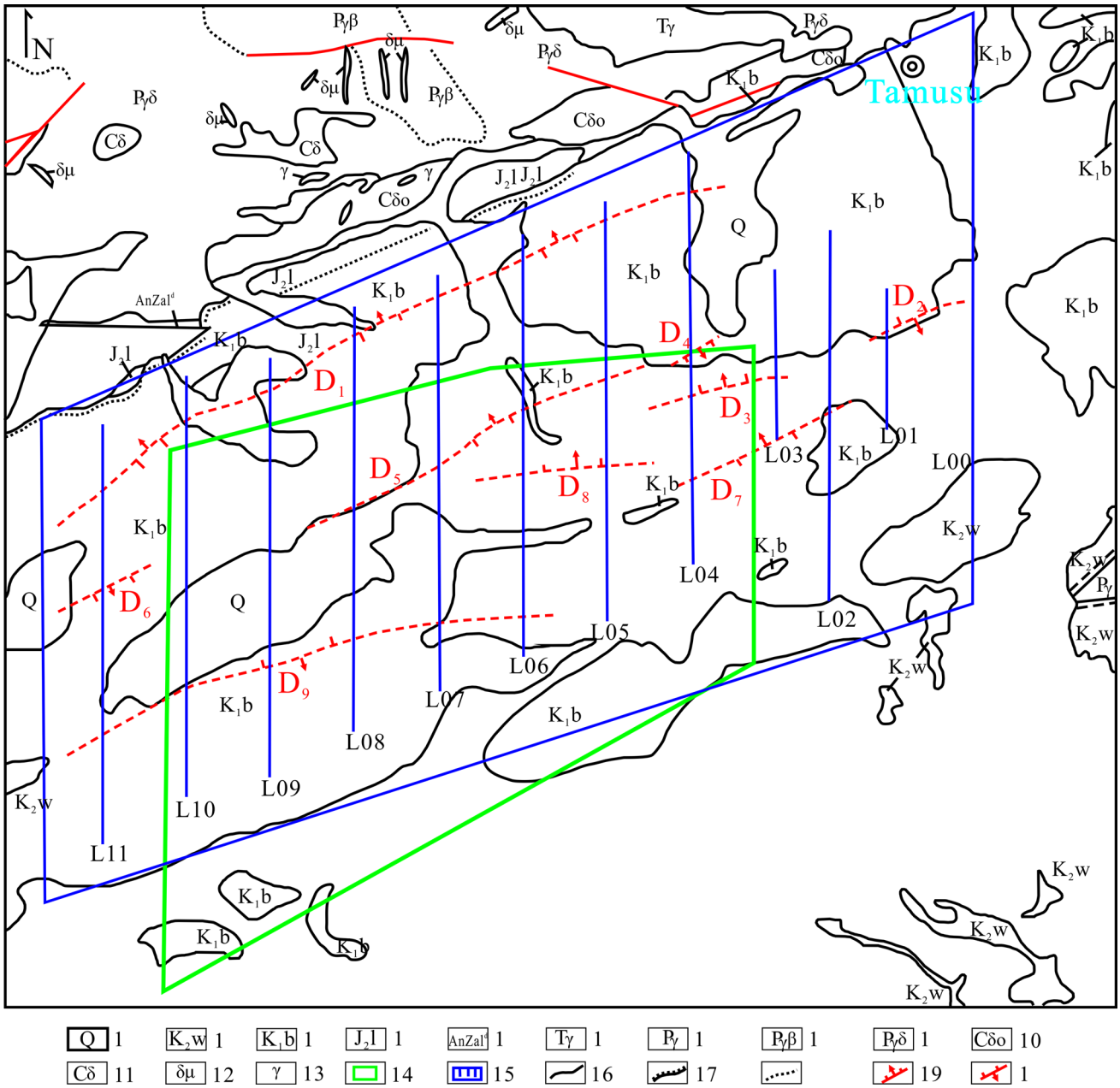

Fig. 13 Distribution of faults by seismic exploration in Tamusu [33]. 1-Quaternary; 2-Wulansuhai Formation; 3-Bayingobi Formation; 4-Longfengshan Formation; 5-Alxa Group; 6-Triassic granite; 7-Permian granite; 8-Permian; 9-Permian granodiorite; 10-Carboniferous quartz diorite; 11-Carboniferous diorite; 12-Diorite porphyry dike; 13-Granite; 14-Repository pre-selection Lot; 15-Measured geological boundary; 16 Measured angular unconformity geological boundary; 17-Lithofacies boundary; 18-Seismic survey line and working area range; 19-Inferred interpretation of reverse faults; 20-Inferred interpretation of normal faults

strictly follows the distribution direction of the basin and is NE. The deep seismic geological conditions in this area are good, and the physical properties of the reflection interface are very different, which is conducive to the identification of stratigraphic information and structural development characteristics in this area.

In order to further comprehensively analyze the distribution of earthquakes in the Tamusu section, statistics of

Table 4 The correspondence between seismic reflection interface and strata

Systerm	Series	Formation	Member	Stratum Units	Seismic reflection interface and code
Cretaceous	Upper	Wulanhai Formation		K_2w	T_3 Unconformity interface between Upper Cretaceous and Lower Cretaceous. The incomplete seismic sequence above T3 corresponds to the Upper Cretaceous Wulansuhai Formation (K2w)
	Lower	Bayingobi Formation	Upper	K_1b^2	T_4 The interface between the middle semi-deep lake and the shallow lake in the upper member of the Lower Cretaceous Bayinggobi Formation
					T_5 The largest lake flooding surface in the Lower Cretaceous sequence is the sand-mud interface commonly found in the upper member of the Bayinggobi Formation
					T_6 The interface between the upper and lower members of the Lower Cretaceous Bayingobi Formation
			Lower	K_1b^1	T_7 The interface between the alluvial fan deposits and the shallow lacustrine facies deposits filled in the early stage of the Lower Cretaceous Bayinggobi Formation
					Tg The unconformity interface between the Cretaceous and the overlying Jurassic, Paleozoic and granites is the bottom Cretaceous interface
Jurassic and Paleozoic				J + Pz	

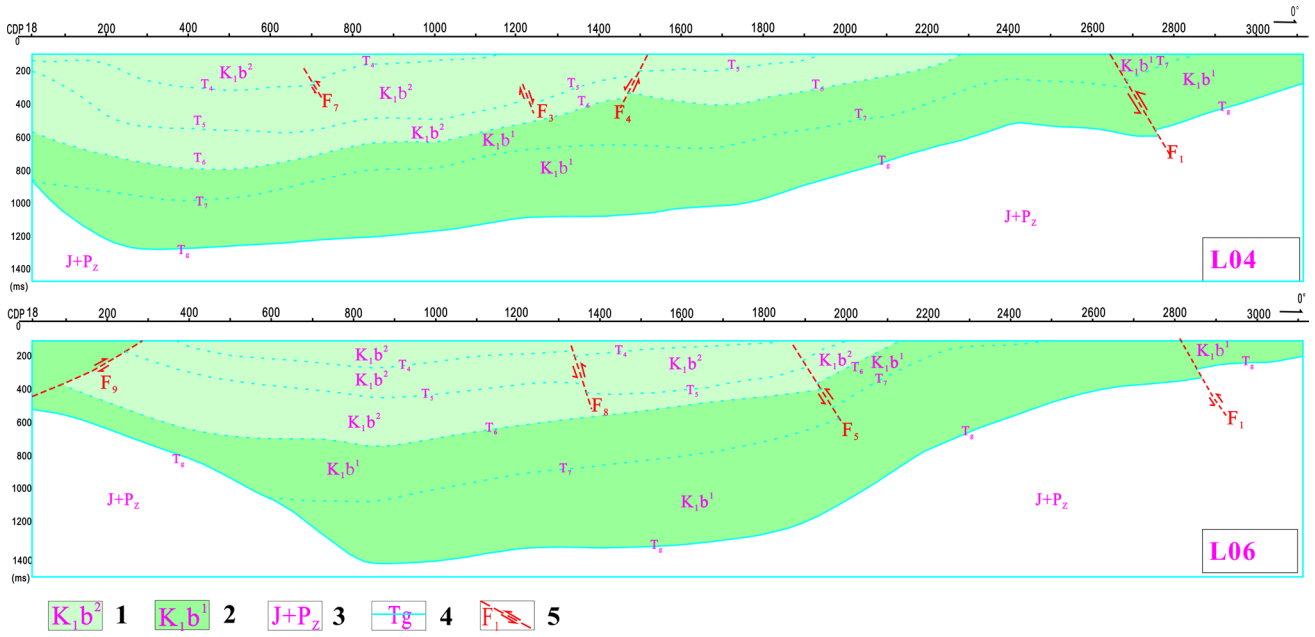

Fig. 14 Fault interpretation of shallow seismic exploration profile in Tamusu area. 1-Upper member of Bayingobi formation of Lower Cretaceous system; 2-Lower member of Bayingobi formation of Lower Cretaceous system; 3-Jurassic and Paleozoic; 4-Stratigraphic interface and number of inferred interpretation; 5-Inferred and interpreted faults and numbers

earthquake history records show that there are more than 870 earthquakes with a magnitude of ML ≥ 3 in the preselected section and surrounding areas. The distribution of earthquake epicenters in the study area is very heterogeneous in space. In seismically active regions, the distribution of earthquakes is also non-uniform, and they

Table 5 Shallow seismic exploration interpretation faults in Tamusu area

Fault	Through the formation interface	Fault property	Trend	Dip
F_1	T_7, T_g	Reverse	North-East	45°–60°
F_2	T_4	Reverse	South-East	30°
F_3	T_5	Normal	North-East	60°
F_4	T_5, T_6	Normal	South-East	60°
F_5	T_4, T_5, T_6, T_7	Reverse	North-West	50°
F_6	T_7	Normal	South-East	75°
F_7	T_4	Reverse	North-East	50°–60°
F_8	T_4, T_5	Normal	North-West	55°–65°
F_9	T_4, T_5, T_6, T_7, T_g	Reverse	South-East	15°–22°

often occur densely along the fault zone in a distinct band shape (Fig. 15). As can be seen from Fig. 15, although the earthquake occurrence points are densely distributed in the study area of Tamunin and adjacent areas, according to the statistical analysis of the existing data, the largest earthquake with a magnitude of 7.6 in history occurred in the southwest of the study area, which is far from Tamunin. It is located in Gansu, which is more than 300 km away from the study area. The rest of the earthquakes were less than 4 in magnitude, and were 150 km away from the study area, which was relatively far away.

A brief evaluation model

Through the selection of the original data reflecting the geological structure such as boreholes and profiles, a three-dimensional geological model is established according to the required data such as stratigraphic trend, fissure dip angle, and stratigraphic properties. Use Trend Surface, Kriging, DSI and other methods for data interpolation expansion. Import the data into COMSOL, and synthesize the planar geological map and the loaded resistivity section map to form the stratigraphic contour constraints of the 3D geological model. Draw the interface of each layer to generate the layer block. On the basis of the shallow seismic exploration section, the formation blocks are cut and trimmed through Boolean operations, and the parameters such as fracture size, strike, and dispersion are set through the discrete fracture network to generate fractures. Use the split function in the

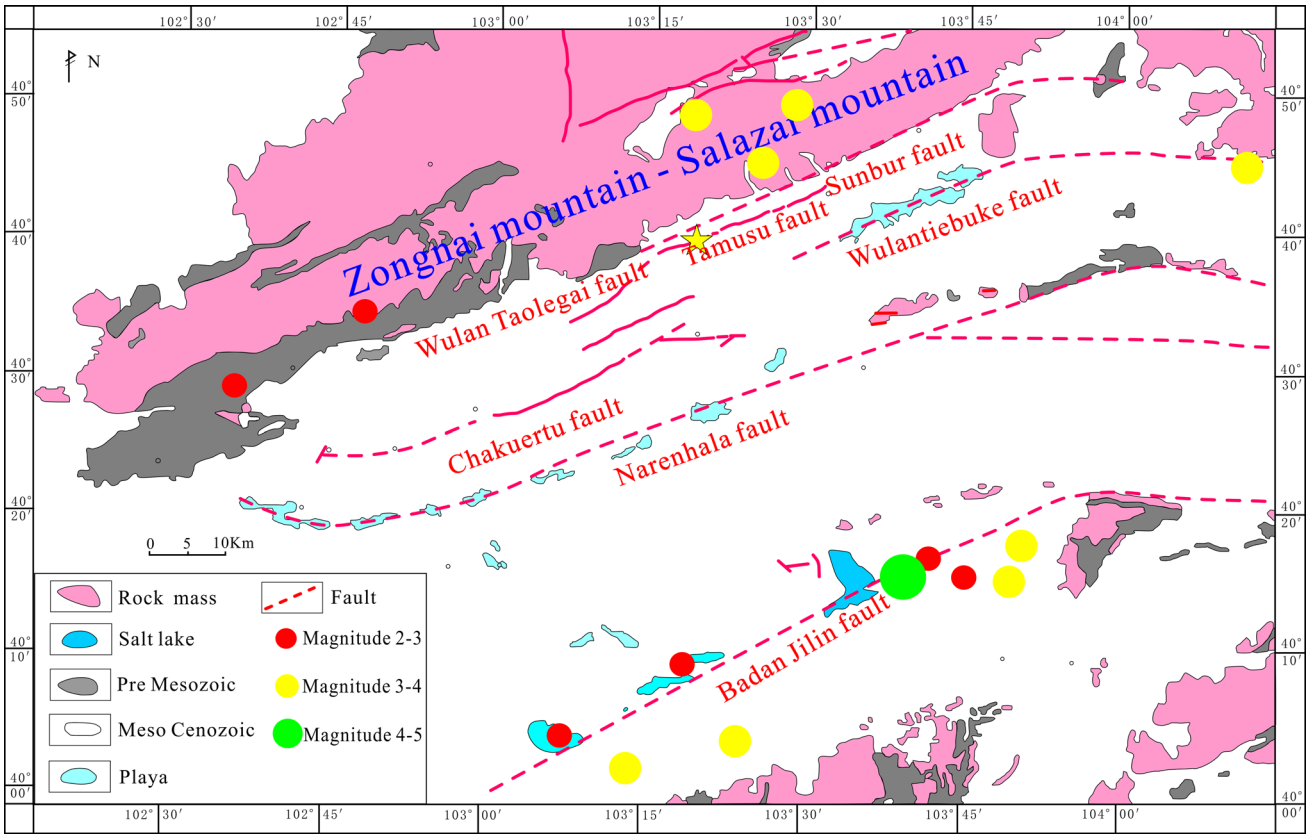

Fig. 15 Statistical distribution map of earthquakes in preselected sections since 1949

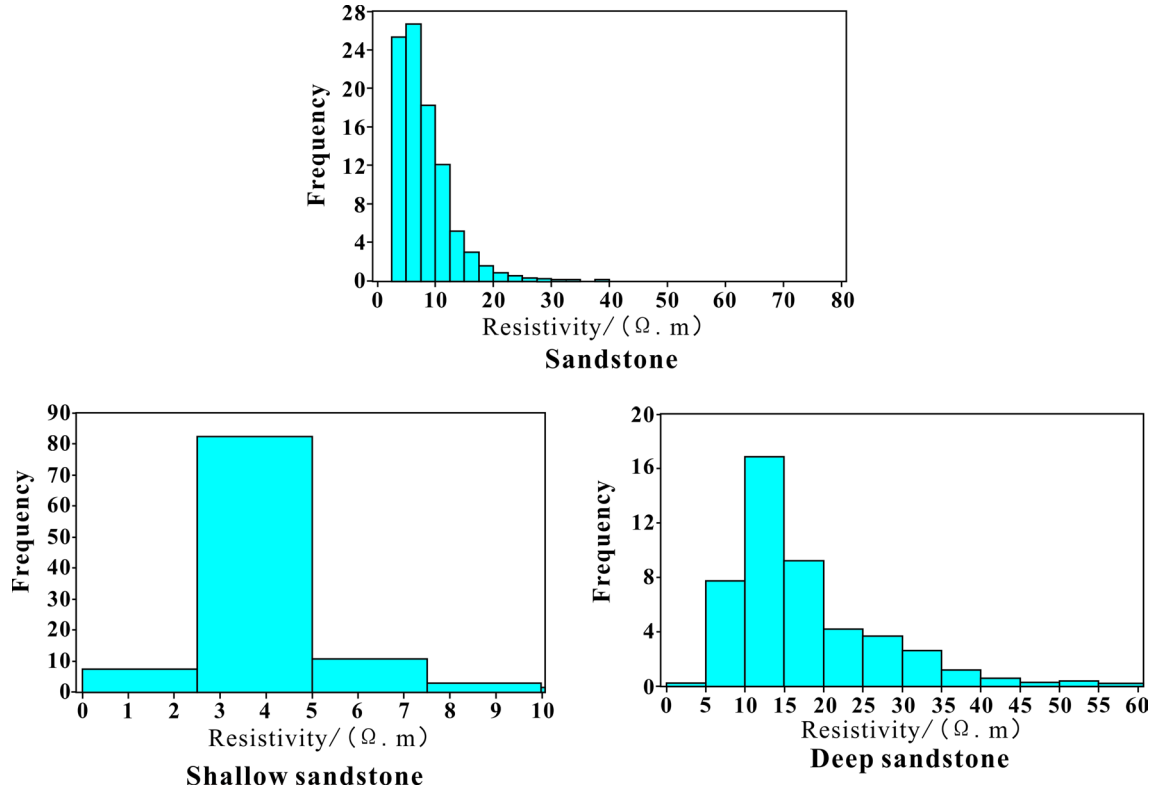

Fig. 16 Statistical histogram of rock resistivity of K_1b^2

geometry to set up fractures penetrating the formation and fine-tune the fracture location.

The data for the establishment of the stratigraphic conceptual model comes from the method of geophysical exploration. Different strata are distinguished according to the physical properties of different rocks, so as to establish a three-dimensional geological model [35, 36]. The resistivity of more than 160 typical rock samples collected from TZK-1 and TZK-2 borehole cores in the preselected section was measured and counted. The resistivity of the K_1b^2 formation is all within the drilling depth of 800 m, and the statistical results are shown in Fig. 16.

According to 10 CSAMT profiles (Fig. 17) in the pre-selected section of Tamusu, the stratigraphic model of the preferred section in the pre-selected section was established. The specific information of the CSAMT survey line is shown in Table 6.

Comprehensive analysis of seismic data and borehole data shows that the geological structure of the pre-selected section of Tamusu is relatively simple. The stratum is divided into three layers from new to old: K_1b^2, K_1b^1 and J + Pz, of which the K_1b^2 stratum is further divided into three layers, $K_1b^{2\text{-}1}$, $K_1b^{2\text{-}2}$ and $K_1b^{2\text{-}3}$, and $K_1b^{2\text{-}1}$ is clay rock (mudstone) for geological disposal of high-level radioactive waste. Key levels of site research. According to the lithology, the model is divided into three layers (Fig. 18), in which the K_1b^2 formation is divided into two layers, and the $K_1b^{2\text{-}2}$ and $K_1b^{2\text{-}3}$ layers are used as the first layer. The key layer of $K_1b^{2\text{-}1}$ is used as a single layer. The K_1b^1 formation and the basement formation J + Pz without the comparison of drilling data are taken as the third layer.

It can be seen from Fig. 18 that the $K_1b^{2\text{-}1}$ stratum as the key target horizon has stable lithology, continuous deposition, thick deposition thickness and small variation in deposition depth. The geological features displayed by the model are in good agreement with the stratigraphic features described by the geological data, indicating that the established geological model can more accurately display the spatial distribution characteristics of each stratum in the preselected section.

According to the geological data of the pre-selected section, the plan geological map, and the shallow seismic exploration section (Fig. 19), the fault model is constructed, and the three-dimensional model of each fault in the pre-selected

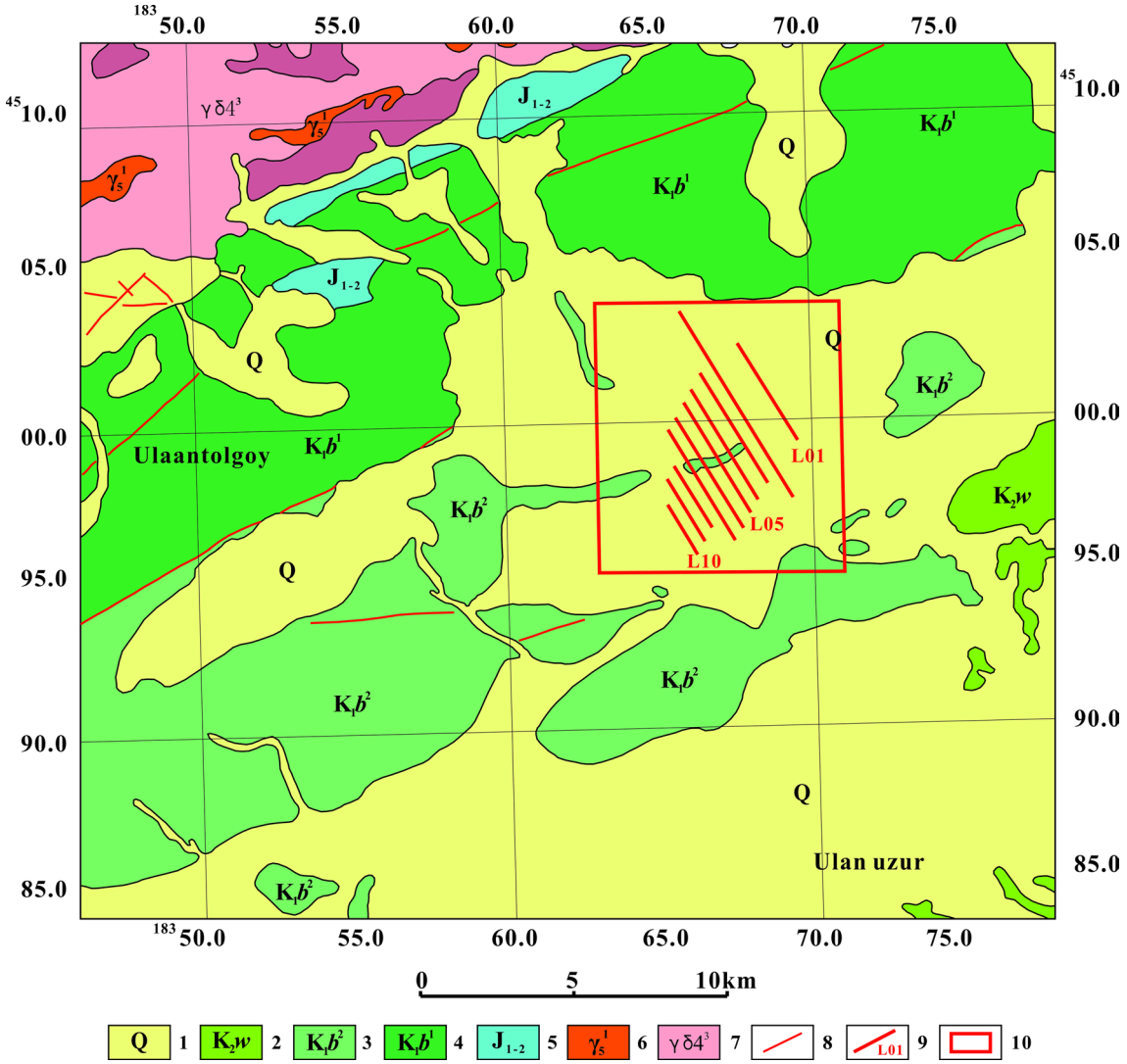

Fig. 17 CSAMT survey line layout of preselected candidate sector. 1-Quaternary; 2-Wulansuhai formation; 3-Bayingobi formation Upper member of Lower Cretaceous; 4-Bayingobi formation Lower member of Lower Cretaceous; 5-Middle lower Jurassic; 6-Indosinian granite; 7-Late Variscan granodiorite; 8-Measured fracture Late; 9-CSAMT survey line and number; 10-Preselected region

section is established by combining all the information of each fault (Fig. 20). Finally, it is superimposed with the stratigraphic model to obtain the three-dimensional geological model of the preselected section.

The three-dimensional geological model is based on the stratigraphic characteristics, shallow seismic profiles and fault structures of the Tamusu study area, and uses the corresponding modeling methods to three-dimensionally display the structural shape, stratigraphic relationship, structural development and internal structure of the geological body. The visualization of the 3D geological structure model of the study area is realized. The three-dimensional scene of the main geological bodies and structural interfaces in the pre-selected section of Tamusu and its surrounding areas is simulated, and the three-dimensional spatial distribution of the pre-selected section of the clay rock high-level radioactive waste repository is visually displayed. It provides a decision basis for further development of the underground space distribution of geological bodies in the pre-selection area and the construction of high-level radioactive waste repositories.

Table 6 CSAMT survey line information table in Tamusu candidate sector

Line number	Length (km)	Trend (°)	First coordinate of survey line		Line tail coordinates	
			L	B	L	B
L01	3.6	330	103.452925	40.615811	103.431017	40.643600
L02	6.8	330	103.450715	40.601154	103.409327	40.653633
L03	4.05	330	103.419948	40.635147	103.419644	40.635533
L04	4.05	330	103.417179	40.631169	103.441839	40.599919
L05	4.05	330	103.439063	40.595947	103.414402	40.627197
L06	4.05	330	103.436597	40.591588	103.411935	40.622837
L07	4.05	330	103.433522	40.587998	103.408862	40.619246
L08	2.25	330	103.424664	40.591738	103.410967	40.609098
L09	2.25	330	103.421895	40.587761	103.408194	40.605122
L10	1.8	330	103.419100	40.583800	103.424777	40.597674

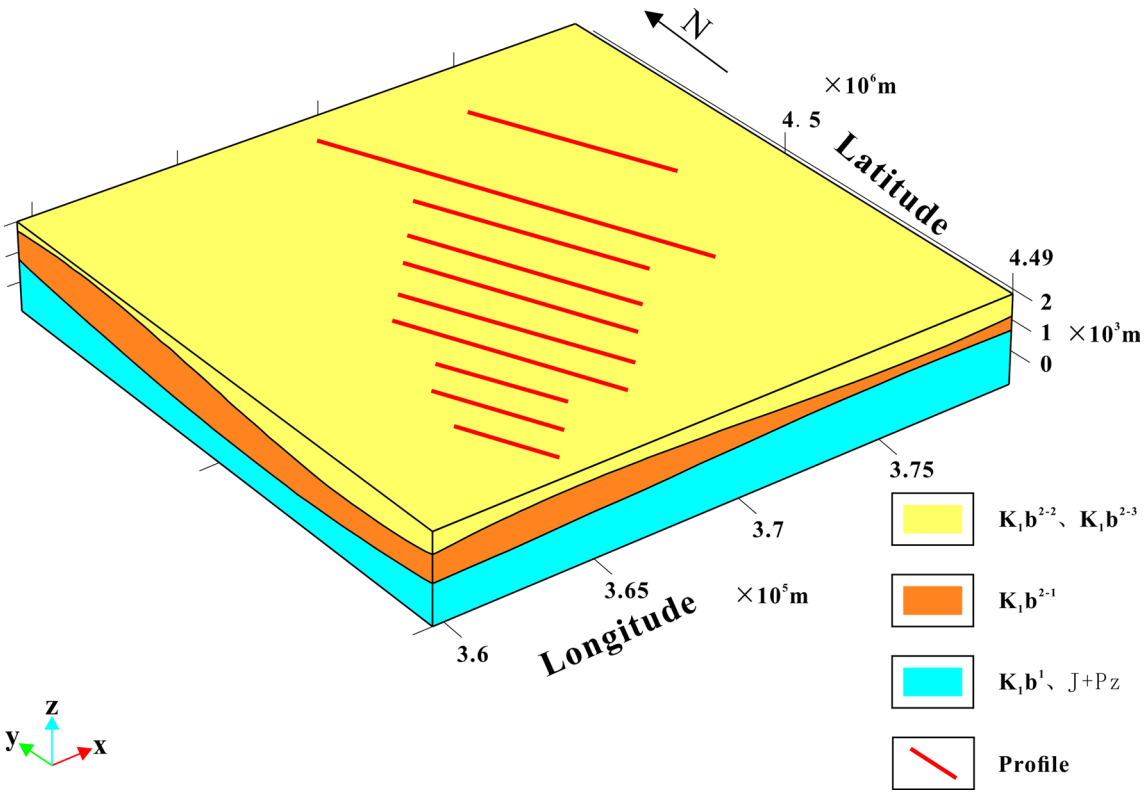

Fig. 18 3D Stratigraphic model of candidate sector [37]

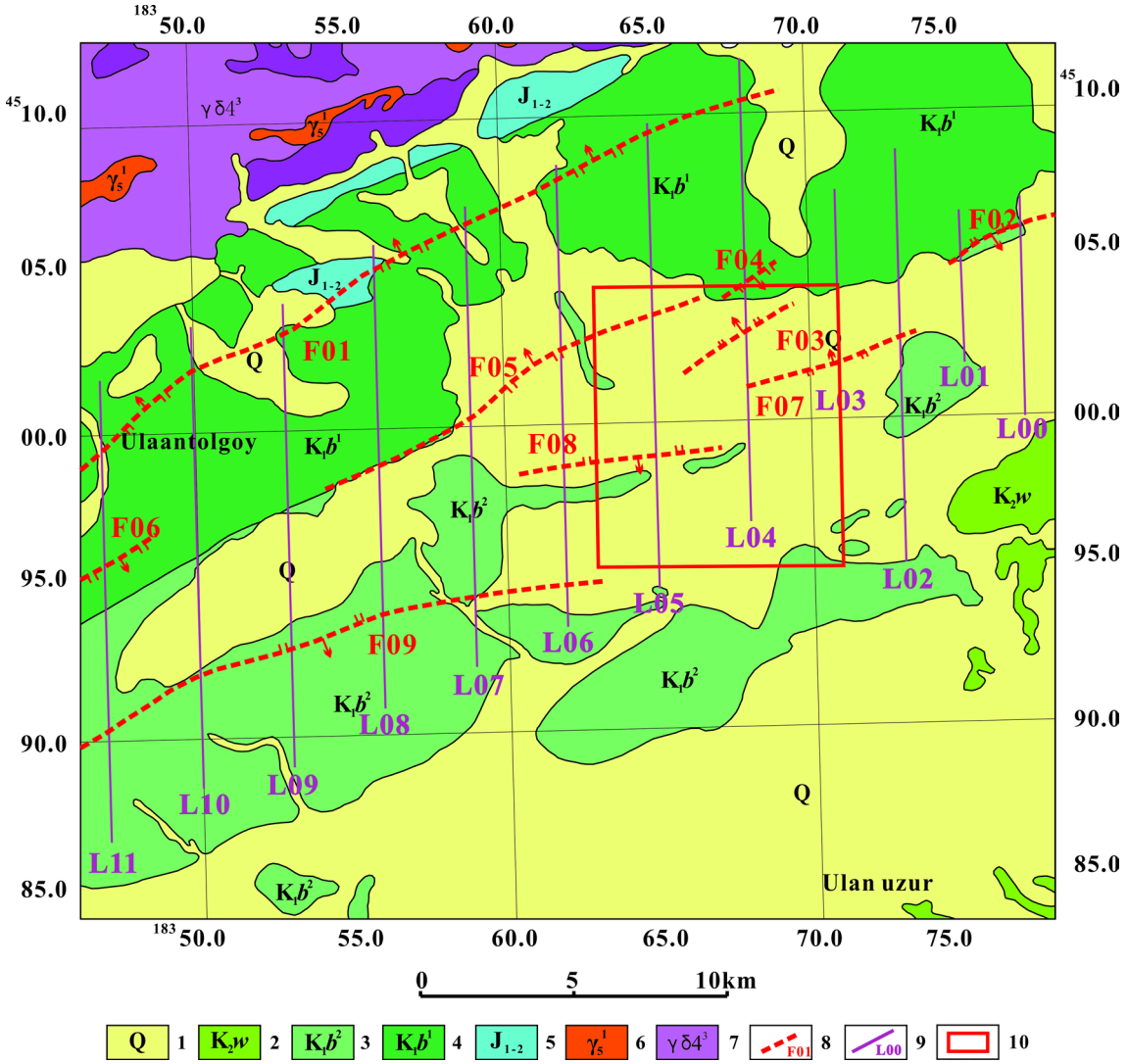

Fig. 19 Plane distribution of shallow seismic profile in candidate sector. 1-Quaternary; 2-Wulansuhai formation; 3-Bayingobi formation Upper member of Lower Cretaceous; 4-Bayingobi formation Lower member of Lower Cretaceous; 5-Middle lower Jurassic; 6-Indosinian granite; 7-Late Variscan granodiorite; 8-Measured fracture Late; 9-Shallow seismic profile; 10-Preselected region

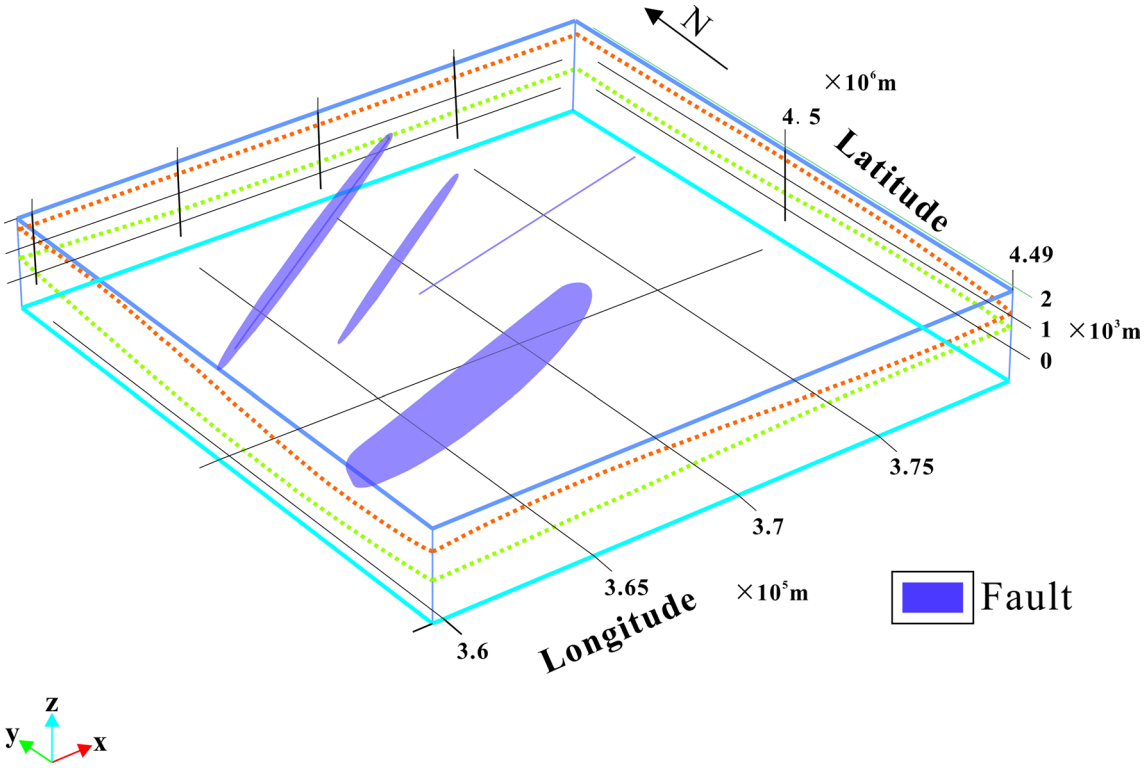

Fig. 20 3D model of fault in candidate sector [37]

Conclusion

The activity of the fault structures in the Tamusu area since the Quaternary affects the stability of the regional tectonic environment. The possible future changes or development trends such as crustal stability are of great significance for the screening of high-level radioactive waste clay rock repository sites. Through the comprehensive analysis and model construction of the topography, stratum characteristics, tectonic geology and fault activity in the Tamusu area, the following understandings are obtained:

1. The sedimentary system in the Tamusu area is mainly composed of fan delta, braided delta and lacustrine sediments. Among them, the lacustrine sediments have a large area and are mainly distributed in the sedimentary centers of each secondary depression. The lithology is mainly gray and dark gray silty mudstone, mudstone intercalated with fine sandstone and siltstone. At the same time, lacustrine deposition is also an important condition for the formation of clay rocks in this area.
2. Analyzing the fault activities distributed in the Tamusu section and nearby areas since the Quaternary, the main faults are relatively stable, which reflects that the tectonic environment of this section has been stable since the late Quaternary, and the crust is in a stable state.
3. From the dislocation analysis of the Tamusu fault, it can be seen that since the formation of the Quaternary river terrace, the activity of the Tamusu fault has been weak, and the fault structure has developed, but all of them are passive faults. Although there are earthquake occurrence points, they are all located in the adjacent areas of the Tamusu study area. It has little effect on the screening of favorable sites for the high-level radioactive waste clay rock repository site.

Acknowledgements We would like to express sincere thanks to Dr. Shuiwei Zhao from China Institute for Radiation Protection for his helpful discussion on criterion analysis. Prof. Miles Silbeman from University of Texas at El Paso is highly acknowledged for his help on grammar correction and professional comments that helps improving this paper to a higher level. This work was funded by the National Defense science, Technology and Industry Bureau project (NO. [2014]1587), Independent Fund Projects from the State Key Laboratory of Nuclear Resources and Environment (No. Z1904), and Special funds for local science and technology development guided by the central government (No. 2018ZDB40001), and Joint Innovation Fund of China Uranium Co., Ltd. - State Key Laboratory of Nuclear Resources and Environment, East China University of Technology (2022NRE-LH-01) and National Natural Science Foundation of China (42302044).

Data availability All data, models, and code generated or used during the study appear in the submitted article.

Declarations

Conflict of interest The authors declare no conflict interest.

References

1. Laurence SC (1997) Site selection and characterization processes for deep geological disposal of high-level nuclear waste. Albuquerque Sandia National Laboratories
2. Pan Z, Qian Q (2009) Research on geological disposal strategy of high level radioactive waste. Atomic Energy Press, Beijing, pp 15–17
3. IAEA (1997) Experience in selection and characterization of sites for geological disposal of radioactive waste. Technical Report No. 991, Austria
4. IAEA (2003) Scientific and technical basis for the geological disposal of radioactive waste. Technical Report Series No. 413
5. IAEA (2006) IAEA safety standards series no. SF-1, fundamental safety principles, safety fundamentals. IAEA, Vienna
6. Dossier A (2005) Argile-architecture and management of a geological repository. ANDRA, Paris
7. Liu X, Liu P, Wang C et al (2010) Preliminary sitting of clay formations for HLW geological disposal repository in China. In: Professional Committee of Nuclear Safety and Radiation Environmental Safety of Chinese Society of Environmental Sciences. Proceedings of the 3rd symposium on underground waste disposal, p 11
8. Che S, Liu X, Liu P (2011) Research of claystone in Longdong area Gansu province. J East China Univ Technol (Nat Sci Ed) 34(02):111–116
9. Ding H, Liupinghui (2015) Geological characteristics of argilaceous rocks in Nanbaxian area of northwest Qaidam basin. Energy Res Manag 2015(02):87–92. https://doi.org/10.16056/j.1005-7676.2015.02.021
10. Zhao S, Li H, Cui Z et al (2016) Investigation on social and economic conditions of preselected area in Longdong Region for HLW geological disposal repository of clay formations. Environ Sci Manag 41(10):12–16
11. Tang Y, Wen Z, Zhang C et al (2007) Geochemical characteristics and origin of oil sand of Tian 2 Well, Tiancao Sag. Bull Geol Sci Technol 2007(04):47–52
12. Li X (2010) Sedimentary facies analysis of the upper part of the Bayingobi formation in the Tamusu area of the Bayingobi basin. J Henan Polytech Univ (Nat Sci) 29(S1):177–180. https://doi.org/10.16186/j.cnki.1673-9787,2010.s1.016
13. Liu X, Liu P (2012) Research on the basic characteristics of clay rock in Tamusu area of Bayingobi Basina. In: Professional Committee of Nuclear Safety and Radiation Environmental Safety of Chinese Society of Environmental Sciences. Proceedings of the 3rd symposium on underground waste disposal, p 9
14. Guan W, Liu X, Liu P (2014) Study on the geological characteristics of claystone in Tamusu area of Bayingebi Basin. World Nucl Geosci 31(02):95–102
15. Zhang Y (2016) Study on clay formation of Upper Bayingebi formation in Tamusu candidate area-high-level radioactive waste disposal repository. East China University of Technology, Nanchang
16. Wang F, Hou S, Zhang L et al (2018) Study on the characteristics of water-rock interaction and its relation to uranium mineralization in Tamusu Uranium Deposit, Southern Bayin Gobi asin. Geol Rev 64(03):633–646. https://doi.org/10.16509/j.georeview.2018.03.009
17. Peng Y, Wang Q, Dai M et al (2018) Ore body spatial distribution characteristics of TMS uranium deposit and prospecting prediction in Bayingebi basin. World Nucl Geosci 35(03):131–136
18. Wei S, Zhang H, Chenqilin (2006) Petroleum geological characteristics and exploration prospects of Yingen-Ejina Banner Basin. Petroleum Industry Press, Beijing
19. Lu J, Chen G, Wei X et al (2011) Post-sedimentary tectonic evolution, cap rock condition and hydrocarbon information of Carboniferous-Permian in Ejin Banner and its vicinities, western Inner Mongolia: a study of Carboniferous-Permian petroleum geological conditions. Geol Bull China 30(6):838–849
20. Huang H (2013) Tectonic framework and regional evolution characteristics of the upper Palaeozoic in Yin-E basin a case study in Ju Yanhai depression. Yangtze University, Jingzhou
21. Long Y (2014) Research on crustal stability of Xinchang and Jiji tank preselected sites for high-level radioactive waste repository. Beijing Research institute of Uranium Geology, Beijing
22. Han W (2017) Study of sedimentary-tectonic evolution since late paleozoic and its impacts on oil and gas geological conditions of Yin-E basin. Northwest University, Xi'an
23. Wu R, Zhou W, Liu P et al (2008) Analysis of metallogenic condition and prospecting potential of sandstone type uranium deposit in Tamusu district of Bayinggebi basin. Uranium Geol 24(1):24–31
24. Zhang D, Fu G, Qin E et al (2002) Jurassic palaeoclimate, Palaeovegetation and palaeoenvironment in the Tuha basin in Xin-Jiang. Geoscience 2002(02):147–152
25. Wang T (1993) Late Paleozoic extension and Tectono-Magmatic evolution in the sino-mongolia border region in the northern part of Alxa. Geol Bull China 1993(04):317–327
26. Chen Q, Wei P, Yang Z (2006) Tectonic evolution and petroleum prospection in the Yin'gen-Ejina Basin. Pet Geol Exp 2006(04):311–315
27. Li Y (2006) The application of the seismic coherence technique to the interpretation of faults and sedimentary facies in the Shengli Oil Field. Sediment Geol Tethyan Geol 2006(03):67–71
28. Zhang C, Nie F, Hou S et al (2015) Ore-controlling factors and metallogenic model of Tamusu sandstone type uranium deposit in Bayingobi Basin, Inner Mongolia. Bull Geol Sci Technol 34(01):140–147
29. Liu B, Zhao C, Ying G et al (2008) The Characteristics of the Laoyachen Fault in Zhenzhou receaaled by shallow seismic date of P wave end S wave. Seismol Geol 2008(02):505–515
30. Wang Y, Meng G, Chai C et al (2015) The accurate location methods for buried active fault exploration: an exploration of Luhuatai Faults in Yinchuan graben. Seismol Geol 37(01):256–268
31. Rao Z (2018) Tectonic activity of Tamusu candidate area in Alxa Youqi, Inner Mongolia: a case study of the Tamusu fault. East China University of Technology, Nanchang
32. Wang L, Li H, Xu G et al (2004) Shallow seismic exploration report in Tamusu area, Alxa Right Banner, Inner Mongolia. Nuclear Industry Aerial Survey and Remote Sensing Center
33. Liu B, Wei B, Li Y et al (2014) Shallow seismic exploration in southwest Tamusu area of Alxa Right Banner, Inner Mongolia. Center Airborne Survey and Remote Sensing Center of Nuclear Industry
34. Huo L, Zhang J, Zhen L et al (2014) Fault interpretation with multiple attributes in coalbed methane interpretation. Oil Geophys Prospect 49(S1):221–227+10. https://doi.org/10.13810/j.cnki.issn.1000-7210.2014.s1.041.
35. Wu Q, Xu H (2004) Research on 3D geological modeling and visualization method. Sci Sin (Terrae) 2004(01):54–60

36. Xu W (2019) Applied research of comprehensive geophysical and three dimensional geological modeling in site evaluation of geological disposal repository of high-level radioactive waste. East China University of Technology, Nanchang
37. Rao Z (2021) Preliminary adaptability assessment on Tamusu Mudstone candidate sector for high-level radioactive waste geological disposal repository. East China University of Technology, Nanchang. https://doi.org/10.27145/d.cnki.ghddc.2021.000002